CANADIAN JOURNAL OF REMOTE SENSING
2017, VOL. 43, NO. 1, 16–27
http://dx.doi.org/10.1080/07038992.2017.1252907

Taylor & Francis
Taylor & Francis Group

Layer Stacking: A Novel Algorithm for Individual Forest Tree Segmentation from LiDAR Point Clouds

Elias Ayrey[a], Shawn Fraver[a], John A. Kershaw Jr.[b], Laura S. Kenefic[c], Daniel Hayes[a], Aaron R. Weiskittel[a], and Brian E. Roth[d]

[a]School of Forest Resources, University of Maine, 5755 Nutting Hall, Orono, ME 04469-5755, USA; [b]Faculty of Forestry and Environmental Management, University of New Brunswick, PO Box 4400, 28 Dineen Drive, Fredericton, NB E3B 5A3, Canada; [c]US Forest Service, Northern Research Station, Bradley, ME 04411, USA; [d]Cooperative Forest Research Unit, University of Maine, 5755 Nutting Hall, Orono, ME 04469-5755, USA

ABSTRACT

As light detection and ranging (LiDAR) technology advances, it has become common for datasets to be acquired at a point density high enough to capture structural information from individual trees. To process these data, an automatic method of isolating individual trees from a LiDAR point cloud is required. Traditional methods for segmenting trees attempt to isolate prominent tree crowns from a canopy height model. We here introduce a novel segmentation method, *layer stacking*, which slices the entire forest point cloud at 1-m height intervals and isolates trees in each layer. Merging the results from all layers produces representative tree profiles. When compared to watershed delineation (a widely used segmentation algorithm), layer stacking correctly identified 15% more trees in uneven-aged conifer stands, 7%–17% more in even-aged conifer stands, 26% more in mixedwood stands, and 26%–30% more (with 75% of trees correctly detected) in pure deciduous stands. Overall, layer stacking's commission error was mostly similar to or better than that of watershed delineation. Layer stacking performed particularly well in deciduous, leaf-off conditions, even those where tree crowns were less prominent. We conclude that in the tested forest types, layer stacking represents an improvement in segmentation when compared to existing algorithms.

RÉSUMÉ

Avec les progrès de la technologie lidar «LiDAR», il est devenu courant pour les ensembles de données d'être obtenus à une densité de points suffisamment élevée pour capturer des informations structurelles d'arbres individuels. Pour traiter ces données, une méthode automatique d'isolement des arbres individuels à partir d'un nuage de points LiDAR est nécessaire. Les méthodes traditionnelles de segmentation d'arbres tentent d'isoler les cimes proéminentes des arbres à partir d'un modèle de la hauteur de la canopée. Nous présentons ici une nouvelle méthode de segmentation, à savoir l'empilage des couches (*layer stacking*), qui tranche tout le nuage de points de la forêt à des intervalles de hauteur de 1 m et isole les arbres dans chaque couche. La fusion des résultats de toutes les couches produit des profils d'arbres représentatifs. Par rapport à la délimitation des bassins versants (un algorithme de segmentation largement utilisé), l'empilage des couches a correctement identifié 15% plus d'arbres dans des peuplements de conifères d'âges inégaux; 7%–17% de plus dans les peuplements de conifères de même âge; 26% de plus dans les peuplements mixtes; et 26%–30% de plus (avec 75% des arbres correctement détectés) dans les peuplements de feuillus purs. Dans l'ensemble, l'erreur de commission de l'empilage des couches est généralement similaire ou meilleure que celle de la délimitation des bassins versants. L'empilage des couches a particulièrement bien performé dans des conditions de feuillus sans feuilles, même celles où les cimes des arbres étaient moins importantes. Nous concluons que, dans les types de forêts testés, l'empilage des couches représente une amélioration de la segmentation par rapport aux algorithmes existants.

ARTICLE HISTORY
Received 20 January 2016
Accepted 3 October 2016

Introduction

Current advances in remote sensing are improving the accuracy and scope of forest inventories by using high-resolution 3-dimensional spatial data. One of the most effective tools for retrieving such data is light detecting and ranging (LiDAR), which uses laser range finding to create 3-dimensional point clouds representing forest canopy structure. Aerial LiDAR applications for forest inventories can be divided into 2 categories. First, *area-based* approaches retrieve general height metrics such as mean point height and point height distributions. These data are used to estimate, for example, forest volume, biomass, and stem density through regression and other modeling techniques (Means et al. 2000; Næsset

CONTACT Elias Ayrey elias.ayrey@maine.edu

2002; Maltamo et al. 2004). Second, *individual-tree-based* approaches first retrieve detailed metrics from individual trees (often directly measuring each tree's crown attributes), then either aggregate them to characterize forest attributes for larger areas, or use them in combination with area-based approaches (Lindberg 2010).

Area-based approaches have been more widely employed than individual-tree approaches, in part because most LiDAR datasets have point densities considered too sparse for the identification of individual tree crowns from point clouds, a process referred to as *segmentation*. However, densities of aerial LiDAR data collections are rapidly improving, with collections regularly flown at densities of ten or more pulses per square meter (pls/m^2), making individual tree segmentation a feasible alternative to area-based approaches. This opens the possibility for identifying and retrieving measurements from all canopy trees over large areas. Some benefits to the individual-tree approach include making the inventory more intuitive (i.e., closely resembling traditional field-based forest inventories but at much larger scales), easier classification of tree species (Vastaranta et al. 2009), and more precise inventories that include listed attributes of each tree, such as height and crown width.

Previous segmentation endeavors show promise yet still highlight the challenge of isolating individual trees. For example, in a comparison across segmentation methods, Vauhkonen et al. (2011) reported individual tree detection rates (defined as percent of trees correctly detected) ranging between 40% and 80% across a variety of forest types. In a similar study, Kaartinen et al. (2012) reported a range between 40% and 90% with boreal conifers. Because of this challenge and variability, few studies have directly compared area-based and individual-tree approaches. Yu et al. (2010) conducted such a comparison and found that the 2 approaches produced comparable mean tree diameters, heights, and volumes, but concluded that the individual-tree approach might yield better results with improved segmentation methods.

Several segmentation methods are currently available, one of the most common being watershed delineation and its variants. This method proceeds by creating a model of the canopy surface (referred to as a canopy height model, CHM), which is inverted to reveal the local maxima ridges that delineate adjacent individual tree crowns (Soille 2009; Chen et al. 2006; Kwak et al. 2007). The method yields favorable results in stands of uniform crown shapes, with distinct peaks and troughs, such as pure even-aged conifer stands; it performs less well when applied to more complex or interlocking crowns, such as those of deciduous stands (Koch et al. 2006). Although standard watershed segmentation, along with other CHM-based segmentation algorithms, is unable to detect overtopped trees (Koch et al. 2014), several variations of watershed delineation show promise in detecting overtopped trees by examining the point cloud beneath the canopy surface. Reitberger et al. (2009) further segmented overtopped trees by identifying their stems using a regression method called RANSAC and then placed nearby points into their appropriate tree by segmenting the watershed into voxels and clumping similar voxels. Duncanson et al. (2014) identified substrata beneath the canopy by subjecting each isolated watershed to further subcanopy watershed delineation.

Although watershed segmentation is currently the most popular method, others are sometimes applied. The local maxima method identifies the peaks of tree crowns and delineates a surrounding crown area by expanding outward from those peaks in a variety of ways, such as valley following or seeded region growing (Wulder et al. 2000, Perrson et al. 2002, Popescu et al. 2002, Popescu et al. 2004).The density-of-high-points method, introduced by Rahman and Gorte (2009), creates a model based on the density of points, analogous to that of a CHM used in watershed delineation. Li et al. (2012) developed a segmentation algorithm that, starting from a local maxima point, iteratively assigns points belonging to that tree based on a distance threshold. Clustering algorithms are also often applied to segmentation, with *k*-means or hierarchical clustering being the most common (Morsdorf et al. 2003; Gupta et al. 2010; Lee et al. 2010). Both show promise for isolating individual trees; however, *k*-means clustering requires prior knowledge of the number of trees present, and hierarchical clustering requires user input or the same knowledge of trees present to decide a stopping point for the clustering process. A further limitation arises when the densest point clusters (assumed to represent the tree center) occur where adjacent crowns interlock.

Here, we present a novel segmentation algorithm referred to as *layer stacking*, which attempts to overcome several of the challenges faced by the algorithms outlined above. Layer stacking involves slicing the forest canopy into layers parallel to the ground, clustering points within each layer, and then stacking the layers to assess cluster location agreements that emerge among layers. The centers of areas of greater agreement are taken to represent the centers of individual trees. The algorithm builds upon concepts implemented in clustering segmentation (Gupta et al. 2010), density-of-high-points scanning (Rahman and Gorte 2009), and local maxima detection algorithms (Popescu 2002). We tested the ability of layer stacking to detect trees by applying it to aerial LiDAR for which we had field-mapped and measured tree data representing a range of tree species compositions and structures. We

also tested layer stacking against a commercially available watershed algorithm and a publicly available local maxima algorithm using these same plots.

Methods

Study area

To assess the accuracy of layer stacking, sites were needed that had a variety of forest stand structures and compositions as well as accurate field-measured tree heights and mapped locations for many individual trees. The sites we selected were located in Maine and New Brunswick's mixedwood Acadian Forest, which support nearly pure coniferous stands similar in structure to boreal forests in northern latitudes, pure deciduous stands similar in structure to the temperate forests of the mid-Atlantic region, and various mixtures of the 2. Three sites were used for algorithm verification. The first was the University of Maine Foundation's Penobscot Experimental Forest (PEF, at 44.879° N, 68.653° W), chosen for the even- and uneven-aged silvicultural treatments applied there by the U. S. Forest Service, Northern Research Station. The second was the University of Maine's Cooperative Forestry Research Unit's Austin Pond (AP, at 45.199° N, 69.708° W) study, chosen for its even-aged silviculture. The third was the University of New Brunswick's Noonan Research Forest (NRF, at 45.988° N, 66.396° W), chosen for its mixedwood forest.

Plots used for verification had previously been established at each site. Plots on the PEF were fixed-area plots of either 15.9 m or 20 m radius with spatial tree measurements taken using a compass and Haglöf Vertex III hypsometer. Plots at AP were 30 m × 25 m and spatial measurements were taken using a Haglöf PosTex Positioning Instrument. Plots at Noonan were 50 m × 50 m, and spatial measurements were taken using gridded tape triangulation. Plot centers were measured via GPS and then were shifted a posteriori to align the tops of trees visually with the LiDAR point clouds. This step was done manually and was necessary prior to assessing the accuracy of any of the segmentation algorithms evaluated in this study. The shifts ranged from 0.6 m to 33.5 m, the magnitude of the shift being a function of GPS accuracy. Plots that could not be visually aligned with the LiDAR were discarded. Trees greater than 11.4 cm diameter at breast height (DBH; 1.37 m) at the PEF and 10 cm DBH at AP and NRF were plotted spatially, with height and species noted. Table 1 lists the attributes and background of each stand. Species composition was noted as the relative frequency of each tree species for plotted trees, and reported down to 5%. Plots with greater than 400 trees per ha were considered to be "dense," whereas those with fewer trees were considered as "sparse." By this designation, the AP site had a high density of trees; however, the uniform tree spacing resulting from precommercial thinning, similar to that of a plantation, resulted in different algorithm performance from the other dense even-aged plots. For this reason, this plot was placed in a separate category.

LiDAR acquisition

Three LiDAR datasets were collected. The first LiDAR acquisition took place in June 2012, with NASA Goddard's LiDAR, Hyperspectral, and Thermal Imager (Cook et al. 2013) over the PEF at an average of 15 pls/m^2, with a pulse rate of 300 Khz, an average footprint size of 10 cm, a 28.5 degree maximum scan angle from nadir, and an altitude of approximately 335 m above ground level (AGL). The second LiDAR dataset was acquired over the PEF and AP in October 2013, in leaf-off conditions with a RIEGL LMS-Q680i at an average of 6 pls/m^2, with a pulse rate of 150 Khz, an average footprint size of 0.17 m, a 28.5 degree maximum scan angle, and at an altitude of approximately 600 m AGL. The 2 PEF datasets were combined visually by aligning easily identified objects. This alignment appeared valid throughout the entire dataset, and trees were not shadowed or distorted. Thus, the final average point density was ~ 21 pls/m^2 over the PEF, and ~ 6 pls/m^2 over AP. The third LiDAR dataset was collected at the NRF under a leaf-off condition in late October 2011, using the same RIEGL LMS-Q680i laser scanner at a pulse density of ~ 5 pls/m^2. The mean flying altitude was 724 m AGL and the maximum scan angle was 28.5 degrees. All LiDAR was collected at a 1550 nm wavelength. Ground points were classified by the provider.

Tree detection

Before segmentation could proceed, we first had to detect the centers of all trees within the stands in question. Raw LiDAR data were first normalized to measure absolute height above ground by subtracting a digital terrain model derived from ground points from each point. Individual forest stands were then separated using a predefined stand map. Each stand was segmented in its entirety, including the plots within.

Each stand selected for segmentation was first horizontally layered at 1-m intervals starting at 0.5 m above the ground and continuing to the highest point (Figure 1a). Clustering algorithms were then applied to each layer. To filter out potentially unwanted low vegetation, the lowest 3 layers were first subjected to Density-Based Scanning (DBScanning), as formulated by Ester et al. (1996). DBScanning classifies points into clusters, based on a density and a minimum number of points per cluster as

Table 1. Stand characteristics of the study area; includes silvicultural history, species composition, and year measured for the 11 stands under study. Stands are grouped by forest type. Stand metrics were based on trees greater than or equal to 11.4 cm DBH. The sites included Penobscot Experimental Forest (PEF), Austin Pond (AP), and Noonan Research Forest (NRF).

Stand Identifier	Density (trees/ha)	Basal Area (m^2/ha)	Silvicultural Treatment	Species/ Composition*	Year Inventoried	Number of Plots
Dense uneven-aged conifers						
PEF-9	510 ± 37	29.2 ± 1.2	Single-tree selection system. Last harvested 2010	35% *Abba*, 33% *Tsca*, 14% *Piru*, 9% *Acru*	2013	4
PEF-16	509 ± 24	25.6 ± 2.1	Single-tree selection system. Last harvested 2012	39% *Tsca*, 38% *Abba*, 9% *Piru*, 7% *Acru*	2011	6
PEF-12	617 ± 27	28.1 ± 1.7	Single-tree selection system. Last harvested 1995	52% *Abba*, 18% *Tsca*, 14% *Acru*, 9% *Piru*	2014	5
PEF-28	564 ± 13	22.9 ± 2.5	Modified diameter limit cutting. Last harvested 1997	43% *Abba*, 18% *Tsca*, 15% *Acru*, 12% *Piru*	2007	4
Sparse uneven-aged conifers						
PEF-15	319 ± 12	7.5 ± 0.7	Fixed diameter-limit cutting. Last harvested 2003	39% *Abba*, 26% *Tsca*, 14% *Piru*, 9% *Acru*, 5% *Bepa*	2007	6
Dense even-aged conifers						
PEF-23B	1434 ± 50	30.3 ± 2.6	Uniform shelterwood, three-stage overstory removal	44% *Abba*, 31% *Pist*, 10% *Tsca*, 10% *Piru*	2011	3
PEF-29B	869 ± 29	17.3 ± 0.7	Uniform shelterwood, 3-stage overstory removal	44% *Piru*, 25% *Abba*, 14% *Pist*, 5% *Bepo*	2011	3
Spaced even-aged conifers						
AP	1332	33.5	Clearcut, followed by precommercial thinning in 1983	79% *Abba*, 11% *Piru*	2014	1
Dense mixedwood						
NRF	1012	43.6	Naturally regenerated following fire	24% *Thoc*, 23% *Acru*, 23% *Piru*, 11% *Abba*, 6% *Beal*, 5% *Bepa*	2015	1
Sparse even-aged deciduous						
PEF-M1	337	21.5	Commercially thinned in 2011, reserve prior	62% *Acsa*, 7% *Acru*, 7% *Osvi*, 5% *Tiam*, 5% *Fram*	2015	1
Dense even-aged deciduous						
PEF-M2	608	45.3	Reserve	66% *Acsa*, 9% *Fram*, 7% *Osvi*, 5% *Tiam*, 5% *Fagr*	2015	1

* Species abbreviations are as follows: Abba = Abies balsamea, Acru = Acer rubrum, Acsa = Acer saccharum, Beal = Betula alleghaniensis, Bepa = Betula papyrifera, Bepo = Betula populifolia, Fram = Fraxinus americana, Fagr = Fagus grandifolia, Osvi = Ostrya virginiana, Piru = Picea rubens, Pist = Pinus strobus, Tiam = Tilia americana, Tsca = Tsuga canadensis, Thoc = Thuja occidentalis.

defined by the user. All points within clusters were thus classified as unwanted low vegetation and removed. All points outside of clusters were assumed to be solitary returns off the narrow tree boles, and were retained.

A canopy height model (CHM) with a resolution of 1 m was then developed over the study areas. This was smoothed with a 3 m × 3 m cell window and local maxima were detected using a 3 m fixed radius window. These maxima were assumed to represent the tops of trees. Each layer was then subject to *k*-means clustering (Figure 1b; Hartigan and Wong 1978), with the local maxima used as seed points. Starting at each of the seed points, *k*-means clustering places points into a cluster belonging to the nearest seed point; the centroid of that cluster is then calculated and used as a new seed point. The algorithm then again clusters all points nearest to each new seed point, repeating the process iteratively until the positions of the seed points no longer

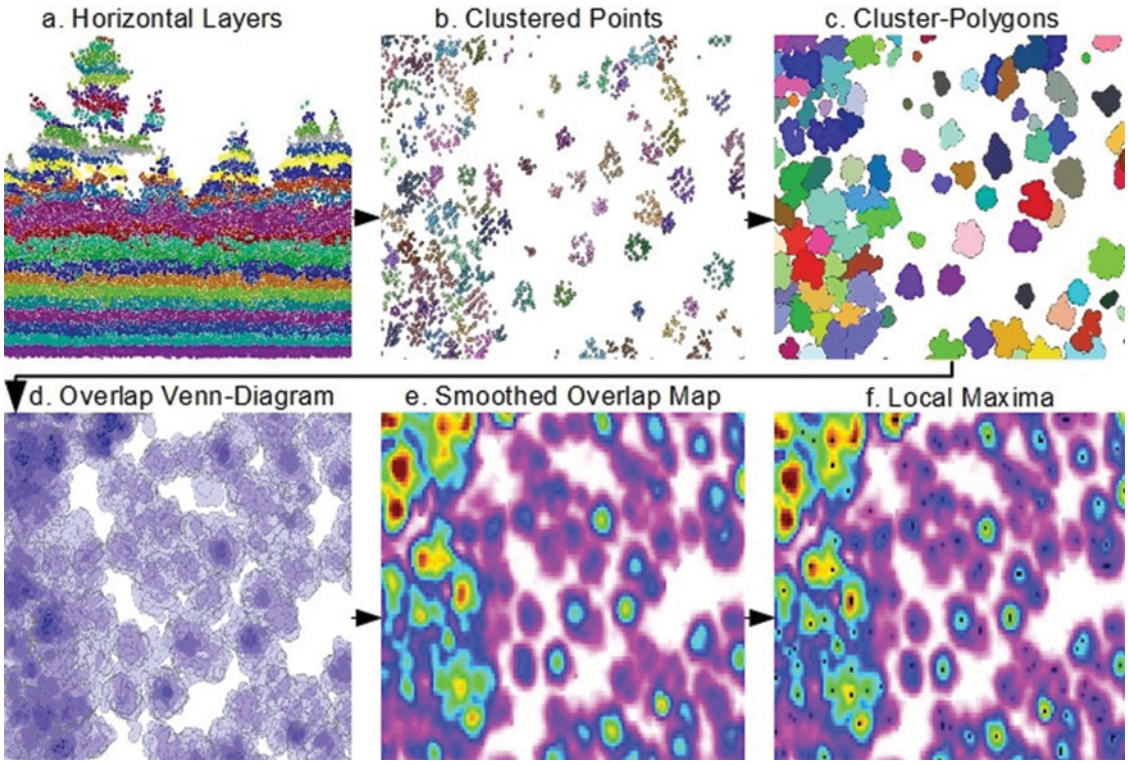

Figure 1. Workflow of the layer stacking tree-detection algorithm. (a) Forest canopy is layered horizontally at 1-m intervals (side view). (b) Points in each layer are clustered; each cluster is assigned a random color (top-down view at 10-m height). (c) Half-meter polygonal buffers are placed around each cluster. (d) Polygons from all layers are stacked on top of one another; areas with darker blue represent more overlap. (e) Areas of overlap between polygons from the different horizontal layers are rasterized and smoothed to produce an overlap map. Areas of increasing warmth (yellow and red) represent greater overlap. (f) Local maxima are detected from the overlap map and displayed as black dots; these are assumed to represent the centers of trees.

change or until a specified number of iterations has been reached.

Once points in each layer were clustered, a 0.5-m polygonal buffer was placed around each cluster (Figure 1c). This step served 2 purposes: first, as an additional round of clustering because points further than 0.5 m from the main cluster, which might have been mistakenly placed into that cluster, were effectively separated from one another; and second, as a means of connecting the points and vectorizing the clusters. The size of this buffer was determined by trial and error after a qualitative visual assessment of tree crowns, and the optimal size could vary slightly by pulse density and forest type. When polygons overlapped in such a way as to form a complete ring around an empty interior, these "donut holes" were filled, because they represented the centers of crowns where the laser could not penetrate. Each layer's polygons were then stacked (Figure 1d), and a rasterized map of the number of overlapping polygons was generated with a resolution of 0.5 m.

In the same way a Venn diagram illustrates areas where 2 or more groups coincide, the overlap map identifies areas of high density in the canopy layers, such that multiple polygon overlaps indicate the presence of an individual tree. In dense conifer stands with little penetration to the center of the tree, additional weight on the overlap map was given to clusters as they near the top of the canopy, because they tended to represent tree apices and, thus, were closer to the tree's center. Clusters in the top 70th percentile were given double weight, the top 80th percentile triple weight, and the top 90th percentile quadruple weight. Thus, in instances of low laser penetration, layer stacking could still function by giving more weight to high points, essentially combining the overlap map and a canopy height model. The overlap map is conceptually similar to the density-of-high-points map developed by Rahman and Gorte (2009), except that the nature of the clustering, as well as the weighting applied to clusters in the upper layers, causes the hollow centers of hard-to-penetrate conifers to be filled in, thus ensuring that the center of these trees truly have the most overlaps (Figure 2).

The overlap map was then smoothed, with a 1.5-m window. This step was needed to remove areas of varying overlap within a tree that might represent branches, in the same way a CHM is smoothed prior to watershed delineation (Koch et al. 2006). Local maxima were then detected with another 1.5-m fixed radius window

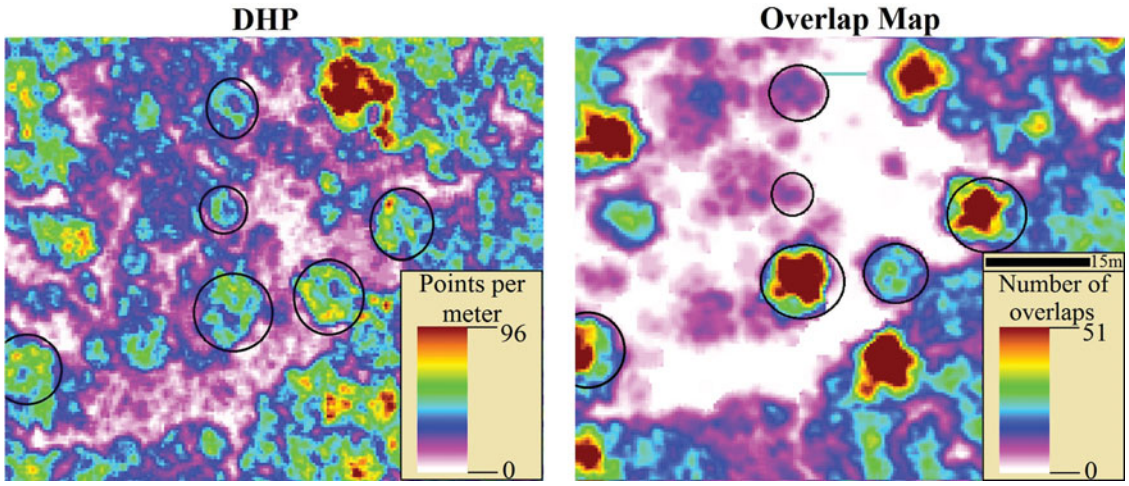

Figure 2. A density-of-high-points map is displayed on the left, whereas an overlap map of a thinned conifer stand is displayed on the right. Areas of increasing warmth (yellow and red) represent higher values. Several trees are circled. Note in the density-of-high-points map the trees form rings, with the areas of highest point density on the outside of the tree. On the overlap map the "donut hole" rings are filled and the highest of cluster-polygons are given more weight, resulting in the densest point, more often being at the center of the tree.

(Figure 1f). These local maxima then were assumed to represent the centers of trees, that is, points that had the most overlapping clusters throughout the canopy. The local maxima detected then had to be filtered for errors. Those that rested atop an area with few overlapping clusters were removed, because they usually represented trees that were of an undesirably small size. For this study, trees with fewer than 5 overlaps were removed, because they tended to represent trees less than 5 m in height and were likely to be below the minimum diameter threshold for field measurement.

Buffers were placed around each local maximum, overlapping buffers were dissolved, and their centroid taken as a new center point for that tree. This step helped to prevent trees from being incorrectly separated into multiple parts, merging local maxima that were too close to one another to be separate trees. We found that a 0.6-m buffer worked well for these data and forest types after a qualitative assessment of several radii options. In very dense stands with small trees, it may be beneficial to reduce this length threshold. The remaining local maxima were assumed to be the centers of trees and were then used for segmentation of individual tree shapes.

Tree segmentation

Tree crowns were assembled using each layer's clustered points. The local maxima derived from the CHM were unable to detect trees in overtopped or intermediate crown classes. Therefore, a second set of clustering was needed, this time using local maxima developed from the overlap map. Because each tree consisted of many layers, the chances of the clustering algorithm yielding erroneous results at one of those layers were high. Therefore, the clustering at each layer was run 3 times, with 3 distinct sets of seed points.

The overlap map was once again smoothed, this time with a 3-m window, a 1.5-m window, and a 0.75-m window. Local maxima were detected using fixed radius windows of the same sizes. These were then used as a series of seed points for 3 separate *k*-means clustering runs. As before, 0.5-m polygonal buffers were placed around each cluster. The polygons in each layer resulting from each of the 3 clustering runs were combined, and duplicate polygons (where the cluster did not change between runs) were removed.

Iterating through each layer, all cluster-polygons that intersected the buffered local maxima developed in the tree detection section were isolated as belonging to that local maxima's tree (Figure 3a). This resulted in assemblages of polygons, each representing the shape of that tree's crown at its respective layer.

Our algorithm includes 3 postdetection error-filtering steps to remove cluster-polygons that did not properly represent the shape of their respective tree. First, cluster-polygons that intersected the cores of 2 trees were eliminated. It was hoped that this step would eliminate the canopy strata above overtopped trees, at the cost of slightly underestimating the size of the dominant tree's crown. Second, cluster-polygon areas so large as to be deemed outliers (greater than 2 standard deviations when compared to other layers within that cluster's tree) were omitted, because these were assumed to represent the erroneous shapes of more than 1 tree. Third, cluster-polygons with centroids far from the local maxima were removed with the assumption being that a correct polygon should be centered over the tree's core. Once again, a

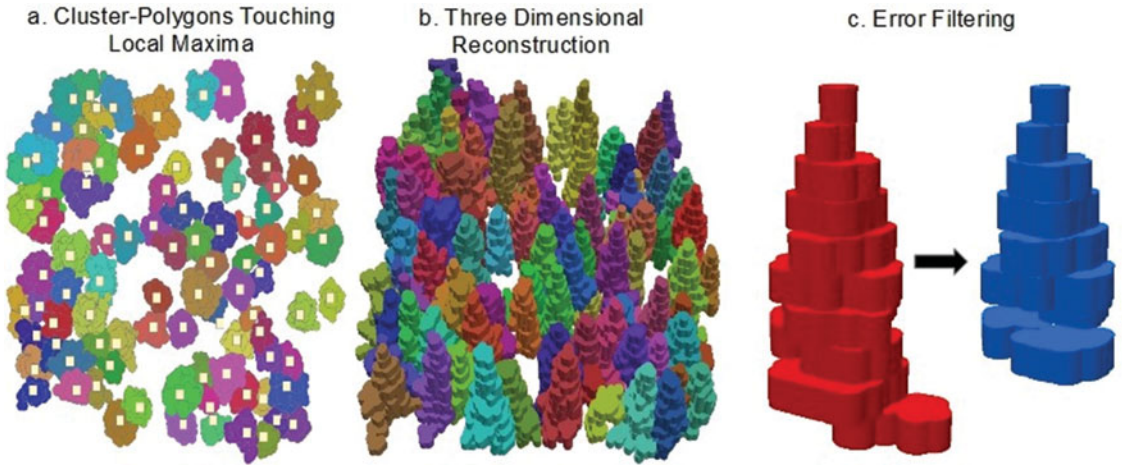

Figure 3. Portions of the layer stacking tree segmentation algorithm, which follows the tree detection steps shown in Figure 1, are illustrated. (a) Local maxima from the overlap map (Figure 1f) are used to delineate cluster-polygons that belong to trees. (b) Three-dimensional reconstruction of each tree's crown shape. (c) Error filtering eliminates mistaken clusters. Note the error filtering inadvertently removed some correct layers, causing a small portion of the tree's crown to be omitted.

2 standard deviation threshold was used to remove polygons with distant centroids (Figure 3c).

The remaining cluster-polygons associated with each tree could be extruded 3 dimensionally back into their original layer so as to approximate the crown shape of each tree (Figure 3b). The core of the tree, represented by the buffered local maxima, was also extruded to the height of the highest tree layer in order to ensure that points representing the tree bole were always captured, and not inadvertently removed in the filtering process. All points lying within these crown reconstructions (Figure 3b) were then clipped out of the point cloud and assigned a unique tree identification. Unlike watershed delineation, which assigns every point within a given area to a tree, layer stacking leaves many points unclassified, including ground points, low vegetation, saplings, and sometimes missed pieces of tree crowns.

TIFFS watershed delineation

We tested the efficacy of layer stacking against a popular watershed tree segmentation algorithm implemented in the Toolbox for LiDAR data Filtering and Forest Studies (TIFFS; Chen 2007). Raw LiDAR data from each plot were input into TIFFS, and the shape of each delineated crown was used to clip points representing individual trees from the point cloud. Default settings were used in TIFFS, with the exception being that a 0.5-m fixed radius window was used to smooth the surface model after a qualitative analysis of several radii.

FUSION local maxima delineation

Layer stacking's efficacy was also tested against variable radius local maxima delineation as implemented by the U.S. Forest Service Pacific Northwest Research Station's FUSION v3.50 (McGaughey 2015). The algorithm as implemented in FUSION is similar to that developed by Popescu et al. (2002). Canopy height models were developed at a 0.25-m resolution for the dense stands (PEF-23B, PEF-29B, NRF, and PEF-M2), which was the highest resolution possible, given the LiDAR density, and resulted in the detection of more small trees. A resolution of 0.5 m was used on the other plots, because this seemed to result in fewer commission errors. The CanopyMaxima tool was then used with the default variable radius equation to isolate local maxima and their surrounding minima and to estimate crown width. Buffers the size of each tree's estimated crown width were then placed around the local maxima, and LiDAR points within these buffers were clipped out as individual trees.

Verification

Verification was conducted by comparing the segmented point clouds from all 3 segmentation algorithms, with locations of individually mapped trees from field-measured plots. Points representing delineated trees from each algorithm were assigned random color values by tree number. Detection rates were assessed manually, tree by tree, with field-measured trees plotted in 3-dimensional space as vertical columns extruded to the field-measured height of the tree, with the LiDAR point clouds overlaid. Detection or omission of each tree was noted, and an overall tally of commission errors was made for each plot. Where multiple plots occurred in a stand, stand-level metrics were produced by summing all detected and undetected trees, along with commission errors, in each plot.

Results

Results in the form of detection rate and commission error for each of the algorithms are displayed in Table 2 for each stand and forest type. Results varied dramatically from one forest type to another, and each algorithm performed optimally under different forest conditions.

Layer stacking detected more trees than watershed delineation and local maxima detection in all dense uneven-aged conifer stands, with an average of 15% increase in detection rate compared to watershed delineation, and an average of 30% increase compared to local maxima detection. Layer stacking and watershed delineation had nearly equal average commission errors (26% and 24%, respectively), whereas local maxima detection had considerably fewer commission errors, at 7%. (Table 2).

Detection rate was considerably higher in the sparse uneven-aged stands than in the dense stands, simply because trees in the former were more isolated, which facilitated detection. Both layer stacking and watershed delineation had similar detection rates in this instance. Commission error was noticeably higher for all 3 algorithms in 2 uneven-aged conifer stands (Table 2, stands PEF-15 and PEF-28), possibly due to their field inventories having been conducted 5 years prior to the first LiDAR acquisition. During those 5 years, small trees could have grown beyond 11.4 cm DBH, allowing their detection with LiDAR and not with field data. We believe many of the commission errors noted for all stands and algorithms can be attributed to the detection of small trees (<11.4 cm DBH). Layer stacking detected slightly more trees than did watershed delineation in the dense even-aged stands (11% more, on average), and had lower or nearly equal commission errors than did watershed delineation (Table 2, PEF-23B and PEF-29B). Once again, local maxima detected fewer trees than the other 2 algorithms, but also had far fewer commission errors.

Layer stacking detected 17% more trees than did watershed delineation in the precommercially thinned conifer stand, with nearly equal commission error (Table 2, AP site). This site most closely resembled plantation-like conditions. Point cloud density was 6 pls/m^2 in this stand in contrast to the 21 pls/m^2 used in the PEF. Despite this limitation, the detection rate was relatively high for both watershed delineation and layer stacking (72% and 89%, respectively), likely owing to the structural homogeneity of the stand. Trees with greater horizontal spacing tended to be more easily delineated by both algorithms. Local maxima correctly detected fewer trees than did both algorithms but, again, had fewer commission errors.

The mixedwood stand presented a challenge for all algorithms, and both watershed delineation and local maxima performed quite poorly (Table 2, NRF). This stand had a highly complex vertical canopy structure, without distinct stratification, as well as a diverse, spatially integrated mix of tree species. There were numerous instances of *Acer rubrum* clumps (stems arising from stump sprouts), making both detection and segmentation difficult. Despite this difficulty, layer stacking had a 26% higher detection rate than did watershed delineation, with only 4% more commission errors. Point density was also lower in the dense mixedwood stand (NRF site), at only 5 pls/m^2. This limitation might have contributed to the low detection rates of both watershed delineation and local maxima (Table 2). When segmenting trees with a complex or uneven size structure, more LiDAR returns will likely yield better results, regardless of the algorithm employed.

An important difference in algorithm performance can be seen in the pure deciduous stands, at least in the leaf-off conditions tested here. In the sparse even-aged deciduous stand, layer stacking correctly identified 26% and 24% more trees than TIFFS and FUSION, respectively. Layer stacking's commission error was also less than the other 2 algorithms, with 19% and 12% fewer commission errors than TIFFS and FUSION. Detection rate fell for all algorithms in the dense even-aged deciduous stand; however, once again, layer stacking detected 30% and 40% more trees than the other 2 algorithms. Layer stacking again had fewer commission errors than did TIFFS and FUSION (7% and 10% fewer). As noted, watershed delineation and other CHM-based algorithms might not perform well in deciduous forests with dense interlocking crowns because of a lack of distinct peaks and troughs. Layer stacking, however, appears to perform better under these conditions because it makes better use of laser penetration to the center of the tree. The performance of layer stacking seems to improve when laser returns off the tree bole can be observed at each 1-m layer.

Detection rates also varied by individual tree size. Figure 4 displays detection rates of FUSION, layer stacking, and TIFFS across 2-cm diameter classes for all trees measured. All algorithms detected fewer small trees than large ones, however, layer stacking consistently detected more small trees than did TIFFS and FUSION. Likewise, TIFFS consistently detected more small trees than FUSION.

Discussion

Layer stacking shows promise as a novel method for segmentation, with improved detection rates over traditional watershed delineation and local maxima detection in every stand type and composition we evaluated. We note, however, that in developing the layer-stacking algorithm, several parameters were custom tailored to the specific forest types being tested. In contrast, both the watershed delineation algorithm and the local maxima algorithm

Table 2. Number of trees detected by the Toolbox for LiDAR data Filtering and Forest Studies (TIFFS) watershed delineation, layer stacking, and the FUSION's local maxima is shown for each forest stand, along with detection rate (bold) and commission error. The sites included Penobscot Experimental Forest (PEF), Austin Pond (AP), and Noonan Research Forest (NRF).

		TIFFS				Layer Stacking				FUSION			
Stand Identifier	Number of Trees Measured	Correctly Detected	Total Trees Segmented	Detection Rate	Commission Error	Correctly Detected	Total Trees Segmented	Detection Rate	Commission Error	Correctly Detected	Total Trees Segmented	Detection Rate	Commission Error
Dense Uneven-Aged Conifers													
PEF-9	163	80	99	**49%**	19%	107	145	**66%**	26%	55	55	**34%**	0%
PEF-16	243	125	164	**51%**	24%	165	212	**68%**	22%	82	86	**34%**	5%
PEF-12	171	99	112	**58%**	12%	118	168	**69%**	29%	62	65	**36%**	5%
PEF-28	179	99	152	**55%**	35%	124	167	**69%**	26%	85	101	**47%**	16%
Sparse Uneven-Aged Conifers													
PEF-15	143	109	314	**76%**	65%	112	216	**78%**	48%	84	164	**59%**	49%
Dense Even-Aged Conifers													
PEF-23B	343	240	488	**70%**	51%	265	403	**77%**	34%	119	130	**35%**	8%
PEF-29B	209	152	304	**73%**	50%	186	393	**89%**	53%	88	109	**42%**	19%
Spaced Even-Aged Conifers													
AP	127	91	123	**72%**	26%	113	148	**89%**	24%	53	62	**42%**	15%
Dense Mixedwood													
NRF	252	110	154	**44%**	29%	176	262	**70%**	33%	83	106	**33%**	22%
Sparse Even-Aged Deciduous													
PEF-M1	53	28	54	**53%**	48%	42	59	**79%**	29%	29	49	**55%**	41%
Dense Even-Aged Deciduous													
PEF-M2	79	33	56	**42%**	41%	57	86	**72%**	34%	25	45	**32%**	44%

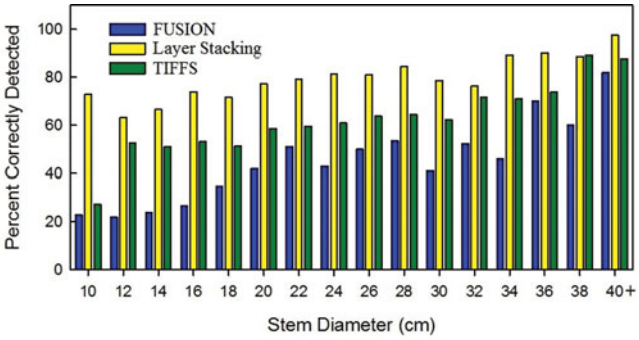

Figure 4. Visual display of detection rates for FUSION, layer stacking, and Toolbox for LiDAR data Filtering and Forest Studies (TIFFS) watershed algorithm are shown below by 2-cm diameter class (DBH rounded to the nearest size class) across all forest types.

were employed with mostly default settings. It is likely that increased accuracy could be obtained from these 2 algorithms by further fine-tuning their many parameters. Despite this caveat, we believe that layer stacking's consistently improved performance over these algorithms indicates that it can serve as a valid alternative for segmentation. Layer stacking, however, has several shortcomings worth noting, which could likely be improved by additional refinements.

First, conifers often yield returns on only the surface of their crowns, leaving a hollow interior. Ideally, the clustering algorithm used in layer stacking corrects for this by grouping all peripheral crown points together and then filling in the center. In practice, however, emergent conifers (mostly *Pinus strobus* in the region tested) could be inadvertently broken into smaller pieces, because the crown perimeters provided more overlaps than did the tree centers. A similar problem occurs in deciduous trees in leaf-on conditions, because fewer laser pulses encounter the tree bole, making detection more difficult. One potential solution is to fly LiDAR with a high scan angle, allowing for more side penetration into the crown, as was done with all LiDAR here. Another solution is to simply fly higher density LiDAR, because more pulse returns would increase the chance of detecting the tree bole.

Second, increases in detection rate must be weighed against the computational inefficiency of layer stacking when compared to watershed delineation. Though computation time and overall efficiency were not recorded, nor were they included in our objectives, we note that layer stacking's computation time increases considerably with plot size or point cloud density. Thus, for small plots, clustering was nearly instantaneous; however, as segmentation area increased to multiple hectares, computation time of the clustering algorithm slowed considerably.

Third, in terms of characterizing crown shape, both layer stacking and watershed delineation need improvement. Because CHM-based segmentation algorithms often mistakenly included smaller trees within or around the crowns of primary trees, we believe they tended to overestimate crown size. However, layer stacking often excluded layers that were farthest from the tree center, which tended to underestimate crown size. The extensive error filtering conducted on each layer had the effect of removing abnormally large clusters, most of which represented the outer portions of the tree crown. When calibrating the error filters for layer stacking, the choice had to be made between full tree crowns, which might have included some erroneous layers of neighboring trees, or narrow crowns, which might have excluded some valid layers. Figure 3c illustrates this trade-off. In the latter case, while the outside canopy envelope might have been slightly clipped, we feel that the shape of the extracted tree's skeletal structure is improved considerably. Whereas watershed delineation extracts every point beneath a blanketed area covered by the tree's canopy, layer stacking selects portions of the tree at each level. Thus, trees were more reliably extracted beneath the surface of the canopy. Beneath the live crown, it is not uncommon for layer stacking to extract only the tree bole and watershed delineation to extract all low-lying vegetation surrounding the tree (Figure 5). The extraction of the bole could prove useful in further analysis, such as stem diameter measurements (Bucksch et al. 2014) or stem-form estimates.

Though tree crown position (dominant, codominant, intermediate, overtopped) was not measured in the field,

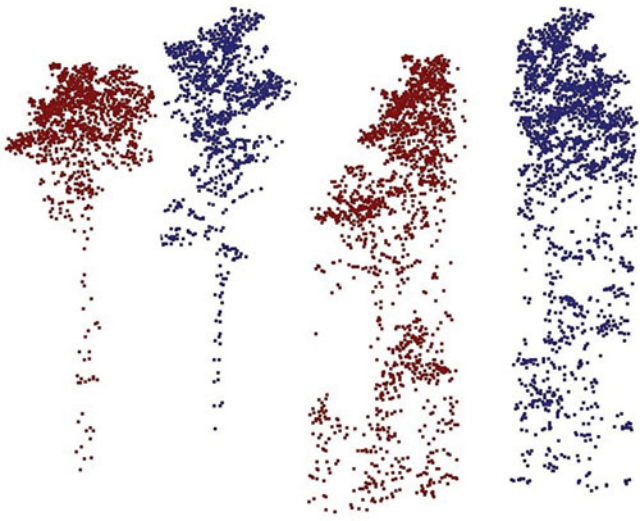

Figure 5. Segmentation results of 2 deciduous trees. The 2 trees on the left were segmented via layer stacking; same 2 trees on the right were segmented via watershed delineation. Layer stacking produced a point cloud that better represents the bole and lower portion of the tree, and watershed delineation segmented every point below the surface, including extraneous features not belonging to the tree.

inferences can be made by examining detection rate of each algorithm by diameter class (Figure 4). As small-diameter trees are more frequently overtopped in most of the uneven aged stands, it can be inferred that layer stacking's noted improvements in detection rate in most stands was due to enhanced detection of intermediate, codominant, and dominant trees. Watershed delineation might have had difficulty segmenting codominant and intermediate trees, which blended in to the watershed profile of larger adjacent trees. An exception to this occurred in deciduous stands, where layer stacking detected more trees in every diameter class. This finding could indicate that layer stacking was better able to detect overtopped trees in these stands. Qualitatively, this appeared to be the case. This could be explained by the greater penetration noted in leaf-off deciduous trees, making the overtopped trees below them visible, and because the canopy above did not block the overtopped tree's signal on the overlap map as it would on a CHM.

Improvement could also be made to the segmentation of overtopped trees. As it stands, detection rate of overtopped trees from the overlap map appears qualitatively high. However, many of those trees were erroneously segmented or filtered out in subsequent steps, and as such, the reported detection rates suffered. In the event that a small tree is detected on the overlap map (signified by few overlaps), it might be beneficial to subject it to further scrutiny, perhaps including only clusters beneath a certain height threshold, or attempting to identify gaps in the vertical strata representing the space between the overtopped and dominant trees, similarly to the method used by Duncanson et al. (2014) with watershed delineation. The use of a variable radius window to detect local maxima on the overlap map may also result in greater detection of overtopped trees, in the same way it increases detection rates on a CHM.

We believe that layer stacking's performance in mixedwood and deciduous stands sets it apart from other CHM-based algorithms, which cannot differentiate between interlocking deciduous tree crowns. Much of layer stacking's performance improvements are likely owed to its use of points below the canopy surface. With multiple returns off the bole of a tree at many layers, a tree's center can be identified even when its crown is not prominent above the canopy, thus giving layer stacking an advantage over algorithms designed to identify trees from a CHM. Ultimately, one must assess the forest type and error tolerance before deciding on a segmentation algorithm. Although local maxima had consistently lower detection rates than both watershed delineation and layer stacking, it also had consistently low commission errors, and might, therefore, be best suited for identifying dominant trees. Likewise, watershed delineation performed nearly as well as layer stacking in sparse and even-aged conifer stands, and given its computational advantage, it could be better suited for large, even, conifer forests. Our results suggest that although layer stacking does perform as well or better than the tested CHM-based algorithms in each tested forest type, it might be best suited for leaf-off forests lacking distinct tree crowns, or situations in which a high level of accuracy is required over a small area.

Conclusions

We developed and tested the layer-stacking algorithm in what we consider to be very challenging forest conditions: mixedwood stands with vertically complex crown structures, including numerous overtopped trees. Despite the areas for improvement discussed, we believe that layer stacking, when applied to these forest types, provides a reasonable alternative to both watershed delineation and local maxima delineation. Improvements were noted in both detection rate and crown shape. Layer stacking appears to be particularly well suited for deciduous leaf-off datasets. We believe layer stacking contributes to the rapidly growing advancements in individual-tree-based approaches in the use of aerial LiDAR data, all hopefully leading to the increased accuracy and efficiency of forest inventories.

Acknowledgments

We thank the U.S. Forest Service, Northern Research Station for providing LiDAR and field data used in this study, and we thank Nicole Rogers in particular for assistance with data access and interpretation. We thank the University of Maine's Cooperative Forestry Research Unit for providing field and LiDAR data for the Austin Pond study site. We thank Bruce Cook and NASA Goddard's G-LiHT team for use of their LiDAR data for the Penobscot Experimental Forest. We thank the Leading Edge Geomatics for use of their LiDAR at the Noonan site. We thank the University of Moncton's Northern Hardwood Research Institute for the use of their TIFFS segmentation software.

Funding

Field measurements were supported by the National Science and Engineering Research Council, Discovery Grant program, and the New Brunswick Innovation Fund, Research Assistants Initiative.

References

Bucksch, A., Lindenbergh, R., Abd Rahman, M.Z., and Menenti, M. 2014. "Breast height diameter estimation from high-density airborne LiDAR data." *IEEEGeoscience and Remote Sensing Letters*, Vol. 11(No. 6): pp. 1056–1060.

Chen, Q. 2007. "Airborne LiDAR data processing and information extraction." *Photogrammetric Engineering and Remote Sensing*, Vol. 73(No. 2): pp. 109.

Chen, Q., Baldocchi, D., Gong, P., and Kelly, M. 2006. "Isolating individual trees in a savanna woodland using small footprint LiDAR data." *Photogrammetric Engineering & Remote Sensing*, Vol. 72(No. 8): pp. 923–932.

Cook, B.D., Nelson, R.F., Middleton, E.M., Morton, D.C., McCorkel, J.T., Masek, J.G., Ranson, K.J., Ly, L., and Montesano, P.M. 2013. "NASA Goddard's LiDAR, hyperspectral and thermal (G-LiHT) airborne imager." *Remote Sensing*, Vol. 5(No. 8): pp. 4045–4066.

Duncanson, L.I., Cook, B.D., Hurtt, G.C., and Dubayah, R.O. 2014. "An efficient, multi-layered crown delineation algorithm for mapping individual tree structure across multiple ecosystems." *Remote Sensing of Environment*, Vol. 154: pp. 378–386.

Ester, M., Kriegel, H.P., Sander, J., and Xu, X. 1996. "A density-based algorithm for discovering clusters in large spatial databases with noise." *Knowledge Discovery in Databases*, Vol. 96(No. 34): pp. 226–231.

Gupta, S., Weinacker, H., and Koch, B. 2010. "Comparative analysis of clustering-based approaches for 3-d single tree detection using airborne fullwave LiDAR data." *Remote Sensing*, Vol. 2(No. 4): pp. 968–989.

Hartigan, J.A., and Wong, M.A. 1979. "Algorithm AS 136: a k-means clustering algorithm." *Journal of the Royal Statistical Society. Series C (Applied Statistics)*, Vol. 28(No. 1): pp. 100–108.

Kaartinen, H., Hyyppä, J., Yu, X., Vastaranta, M., Hyyppä, H., Kukko, A., Holopainen, M., et al. 2012. "An international comparison of individual tree detection and extraction using airborne laser scanning." *Remote Sensing*, Vol. 4(No. 4): pp. 950–974.

Koch, B., Heyder, U., and Weinacker, H. 2006. "Detection of individual tree crowns in airborne LiDAR data." *Photogrammetric Engineering & Remote Sensing*, Vol. 72(No. 4): pp. 357–363.

Koch, B., Kattenborn, T., Straub, C., and Vauhkonen, J. 2014. "Segmentation of forest to tree objects." In *Forestry Applications of Airborne Laser Scanning*, edited by M. Maltamo, E. Næsset, and J. Vauhkonen. Dordrecht, The Netherlands: Springer.

Kwak, D.A., Lee, W.K., Lee, J.H., Biging, G.S., and Gong, P. 2007. "Detection of individual trees and estimation of tree height using LiDAR data." *Journal of Forest Research*, Vol. 12(No. 6): pp. 425–434.

Lee, H., Slatton, K.C., Roth, B.E., and Cropper Jr., W.P. 2010. "Adaptive clustering of airborne LiDAR data to segment individual tree crowns in managed pine forests." *International Journal of Remote Sensing*, Vol. 31(No. 1): pp. 117–139.

Li, W., Guo, Q., Jakubowski, M. K., and Kelly, M. 2012. "A new method for segmenting individual trees from the LiDAR point cloud." *Photogrammetric Engineering & Remote Sensing*, Vol. 78(No. 1): pp. 75–84.

Lindberg, E., Holmgren, J., Olofsson, K., Wallerman, J., and Olsson, H. 2010. "Estimation of tree lists from airborne laser scanning by combining single-tree and area-based methods." *International Journal of Remote Sensing*, Vol. 31(No. 5): pp. 1175–1192.

Maltamo, M., Eerikäinen, K., Pitkänen, J., Hyyppä, J., and Vehmas, M. 2004. "Estimation of timber volume and stem density based on scanning laser altimetry and expected tree size distribution functions." *Remote Sensing of Environment*, Vol. 90(No. 3): pp. 319–330.

McGaughey, R. 2015. *Fusion/LDV: Software for LiDAR Data Analysis and Visualization*, 3.50. Seattle, WA: USDA Forest Service - Pacific Northwest Research Station.

Means, J.E., Acker, S.A., Fitt, B.J., Renslow, M., Emerson, L., and Hendrix, C.J. 2000. "Predicting forest stand characteristics with airborne scanning LiDAR." *Photogrammetric Engineering and Remote Sensing*, Vol. 66(No. 11): pp. 1367–1372.

Morsdorf, F., Meier, E., Allgöwer, B., and Nüesch, D. 2003. "Clustering in airborne laser scanning raw data for segmentation of single trees." *International Archives of the Photogrammetry, Remote Sensing and Spatial Information Sciences*, Vol. 34(Part 3): pp. W13.

Næsset, E. 2002. "Predicting forest stand characteristics with airborne scanning laser using a practical 2-stage procedure and field data." *Remote Sensing of Environment*, Vol. 80(No. 1): pp. 88–99.

Persson, A., Holmgren, J., and Söderman, U. 2002. "Detecting and measuring individual trees using an airborne laser scanner." *Photogrammetric Engineering and Remote Sensing*, Vol. 68(No. 9): pp. 925–932.

Popescu, S.C., Randolph, H.W., and Ross, F.N. 2002. "Estimating plot-level tree heights with LiDAR: local filtering with a canopy-height based variable window size." *Computers and Electronics in Agriculture*, Vol. 37(No. 1): pp. 71–95.

Popescu, S.C., and Wynne, R.H. 2004. "Seeing the trees in the forest: using LiDAR and multispectral data fusion with local filtering and variable window size for estimating tree height." *Photogrammetric Engineering & Remote Sensing*, Vol. 70(No. 5): pp. 589–604.

Rahman, M.Z.A., and Gorte, B.G.H. 2009. "Tree crown delineation from high resolution airborne LiDAR based on densities of high points." In *International Archives of the Photogrammetry, Remote Sensing, and Information Sciences XXXVIII (3/W8)*, *Proceedings ISPRS Workshop Laserscanning 2009*. Paris, France: ISPRS.

Reitberger, J., Schnörr, C., Krzystek, P., and Stilla, U. 2009. "3D segmentation of single trees exploiting full waveform LIDAR data." *ISPRS Journal of Photogrammetry and Remote Sensing*, Vol. 64(No. 6): pp. 561–574.

Soille, P. 2009. "Segmentation." In *Morphological Image Analysis: Principles and Applications*. New York, NY: Springer-Verlag.

Vastaranta, M., Holopainen, M., Haapanen, R., Yu, X., Melkas, T., Hyyppä, J., and Hyyppä, H. 2009. "Comparison between an area-based and individual tree detection method for low- pulse density ALS-based forest inventory." In *Proceedings of Laser Scanning*, edited by F. Bretar, M. Pierrot-Deseilligny, and G. Vosselman, pp. 147–151. Paris, France: pp. 1–2.

Vauhkonen, J., Ene, L., Gupta, S., Heinzel, J., Holmgren, J., Pitkänen, J., Solberg, S., et al. 2011. "Comparative testing of single-tree detection algorithms under different types of forest." *Forestry*, Vol. 85: pp. 27–40.

Wulder, M., Niemann, K.O., and Goodenough, D.G. 2000. "Local maximum filtering for the extraction of tree locations and basal area from high spatial resolution imagery." *Remote Sensing of Environment*, Vol. 73(No. 1): pp. 103–114.

Yu, X., Hyyppä, J., Holopainen, M., and Vastaranta, M. 2010. "Comparison of area-based and individual tree-based methods for predicting plot-level forest attributes." *Remote Sensing*, Vol. 2(No. 6): pp. 1481–1495.